DFT Calculation Analysis of the Infrared Spectra of Ethylene Adsorbed on Cu(110), Pd(110), and Ag(110)

Koichi Itoh,* Tairiku Kiyohara, Hironao Shinohara, Chikaomi Ohe, Yoshiumi Kawamura, and Hiromi Nakai

Department of Chemistry, School of Science and Engineering, Waseda University, Shinjuku-ku, Tokyo 169-8555, Japan

Received: June 6, 2002; In Final Form: July 23, 2002

A density functional theory (DFT) calculation was performed on the cluster models of ethylene on Cu(110), Ag(110), and Pd(110) to clarify the correlation between the IR spectra of the adsorbate and the modes of ethylene−surface interaction. The metal surfaces were modeled by two- or three-layered clusters consisting of 13−34 metal atoms. Four kinds of adsorption sites were considered: atop bonding sites with the CC bond parallel and perpendicular to the $\langle 1\bar{1}0\rangle$ direction (ST and LT sites), a short bridge site with the CC bond parallel to the $\langle 1\bar{1}0\rangle$ direction (SB site), and a long bridge site with the CC bond perpendicular to the $\langle 1\bar{1}0\rangle$ direction (LB site). The results of calculations for three-layered models consisting of more than 20 metals could be compared reasonably with the experimental data. The comparison indicated that (i) upon increasing surface coverage, ethylene on Cu(110) converts its adsorption site from an SB to an ST site, (ii) ethylene adsorbs at an LT site of Ag(110), and (iii) ethylene on Pd(110) takes on an ST site. These conclusions are consistent with those derived from STM and other spectroscopic measurements including UPS and NEXAFS, indicating that the DFT calculation on the cluster models is efficient for the analysis of the IR spectra of ethylene adsorbed on metal surfaces, which delineates the adsorption modes. The contribution of donation and back-donation of electrons to the ethylene−metal bonding was estimated by calculating the projections to the π-bonding and π^*-antibonding orbitals of the isolated ethylene in the adsorbed geometries. The results proved that both the π donation and π^* back-donation make appreciable contributions to the ethylene−surface interaction on Cu(110), whereas the π^* back-donation is negligible in the ethylene−Ag(110) interaction. It was suggested that the frequency increase of the CH_2 out-of-plane wagging vibration from that of the free ethylene observed for ethylene on Ag(110) is a measure of the contribution of the π donation to the ethylene−surface interaction.

1. Introduction

The adsorption mode of ethylene on well-defined transition-metal surfaces has been the subject of considerable interest as a prototype for the interaction of olefinic hydrocarbons with catalysts. Many experimental studies have been conducted to gain insight into the geometric and electronic aspects of the adsorption. Vibrational spectra of ethylene adsorbed on transition metals have provided ample information about bonding modes, adsorption sites, and structures of the adsorbate. In 1988, Shepard[1] wrote an extensive review paper on the vibrational spectra, which had been mainly observed by using high-resolution electron energy loss spectroscopy (HREELS) of ethylene adsorbed nondissociatively at a variety of single-crystal metal surfaces at low temperatures. He concluded that the spectra can be classified in terms of the bonding modes of the adsorbate (i.e., di-σ-bonded (type I) and π-bonded states (type II)). Since then, additional vibrational spectra of ethylene adsorbed on metal surfaces[2,3] has been acquired because of the advent of Fourier transform infrared reflection absorption spectroscopy (FT-IRAS), which can give spectra with a higher energy resolution than HREELS.

In the π-bonded state, the sp^2 hybridization of the free ethylene molecule has been assumed to remain nearly unchanged upon adsorption, whereas the di-σ-bonded state is associated with significant rehybridization toward the sp^3 configuration. These processes have been interpreted in terms of the well-known Dewer−Chatt−Duncanson mechanism,[4,5] which states that attractive interaction between ethylene and metal surfaces could be ascribed to donation and back-donation processes. The donation (hereafter denoted as π donation.) involves a transfer of electrons from a π orbital of the adsorbate to unoccupied metal orbitals, whereas the back-donation (denoted as π^* back-donation) populates a π^* orbital of the adsorbate with electrons from the occupied metal orbitals. These two processes lead to a loss of bond order and thus to an increased C−C bond distance accompanied by partial hybridization toward the sp^3 configuration. The hybridization causes a frequency lowering of the C═C stretching (ν(C═C)) and CH_2 symmetric scissoring (δ_s-(CH_2)) modes of the adsorbed ethylene compared to the frequencies of the free molecule.

To estimate the hybridization as well as the strength of the surface−ethylene interaction on the basis of the frequency lowering, Stuve and Madix[6] introduced the so-called "$\sigma\pi$ parameter". The parameter is obtained from the degree to which the ν(C═C) and $\delta_s(CH_2)$ vibrations are red-shifted below the values for the free ethylene, with an appropriate normalization so that the parameter ranges from zero for the free ethylene to 0.38 for Zeise's salt, which is $Pt-C_2H_4$ and is commonly taken

* Corresponding author. E-mail: itohk@waseda.jp.

10.1021/jp021377p CCC: $22.00 © 2002 American Chemical Society
Published on Web 09/25/2002

as a model for a π-bonded state, to unity for $C_2H_4Br_2$, which is taken as a model for a di-σ-bonded state. Although the parameter is instructive and efficient to the discussion of differences in the coordination mode of ethylene on different metals, quantum chemical calculations should be performed to correlate the vibrational frequencies (or their shifts from those for the free ethylene) to the site of bonding, the structures of the adsorbate, and the relative contribution of the π donation and π^* back-donation to the surface−ethylene interaction.

One of the theoretical approachs along this line has been performed by Wong and Hoffmann,[7] who employed a tight-binding extended Hückel method to trace the adsorption mode of ethylene on transition-metal surfaces, including Ni(111), Pd(111), and Pt(111). They determined the preferred adsorption sites (a di-σ-bonded or a 2-fold bridge site and a π-bonded or atop-bonded site) and the relative importance of the π donation and π^* back-donation to the ethylene−surface interaction. Although these results were supported by the vibrational data obtained by HREELS, the correlation between the mode of adsorption and the vibrational frequencies was discussed only at a qualitative level. In recent years, nonlocal density functional theory (DFT) calculations have been applied to ethylene−metal cluster models to delineate the adsorption mode of ethylene on transition-metal surfaces, including Ni(110),[8] Cu(110),[9,11,12] Cu(111),[10] Ni(111),[11] Ag(110),[12] Pt(110),[12] and Pt(111).[13,14] It has been recognized that the DFT method can reproduce the vibrational spectra of free molecules quite well.[15] The calculated vibrational frequencies of ethylene adsorbed on Ag(110), Cu(110), and Pt(110)[12] by using the DFT calculation method, however, are in a poor agreement with the observed frequencies. This is mainly because the cluster size employed in the calculation is so small that the local potential of ethylene and neighboring metal atoms including the adsorption site is not correctly described because the truncation of the bond on the periphery of the cluster seriously affects the local potential.

The main purpose of the present paper is to simulate quantitatively the vibrational spectra of ethylene adsorbed on Cu(110), Ag(110), and Pd(110) at ca. 80 K by using the DFT calculation method and to clarify differences in the adsorption modes (i.e., the adsorption energy, the adsorption site and structures, and the vibrational frequencies of the adsorbate) among the ethylene/metal surface systems. The vibrational frequencies of ethylene have been accurately determined for the adsorbate on Cu(110),[16−18] on Pd(110),[19] and on Ag(110).[20−22] The adsorption structure of ethylene on Cu(110) has been studied by using UV photoelectron spectroscopy (UPS),[23] photoelectron diffraction,[24] and scanning tunneling microscopy (STM). [25,26] All these studies have shown that ethylene adsorbs on Cu(110) with its CC bond almost parallel to the surface and oriented in the $\langle 1\bar{1}0\rangle$ direction, although ambiguity still exists as to whether the adsorbate takes an atop bonding site or a bridge site. The adsorption structure of ethylene on Ag(110) has been studied by UPS, low-energy electron diffraction (LEED) and thermal desorption spectroscopy (TDS),[27] and near-edge X-ray absorption fine-structure (NEXAFS) measurements,[28] all of which suggested that at 80−110 K ethylene adsorbs on Ag(110) with its CC bond parallel to the surface, taking the π-bonding mode. LEED and TDS have been applied to the study of the adsorption structure of ethylene on Pd(110),[19,29] suggesting that the adsorbate is π bonded to Pd(110) below 280 K. A recent study by STM[30] indicated that the π bonding takes place on top of a Pd atom. Thus, all the studies on the adsorption structures of ethylene on Cu(110), Ag(110), and Pd(110) indicated that ethylene adsorbs molecularly on these surfaces at low temperatures, with the CC bond parallel to the surfaces, taking either a bridge or an atop bonding (or π bonding) site. Although the vibrational spectra of ethylene on Cu(110), Ag(110), and Pd(110)[16−22] can be classified as type II (the π-bonded state) in Shepard's classification,[1] the spectra exhibit appreciable difference depending on the kind of substrate metals used, which can be partly ascribed to the difference in the adsorption site. Therefore, simulating these spectra by using the DFT calculation method can help us to decide how this method can be applied to the determination of the adsorption modes and structures on single-crystal metal surfaces.

The paper is arranged as follows. In section 2, the computational method is described. Employed cluster models are explained in section 3. Section 4 gives the results of calculations, which are compared with the observed data to determine the adsorption site and structures. The contribution of π donation and π^* back-donation to the ethylene−surface interaction is also discussed on the basis of the calculated projection to the π-bonding (HOMO) and π^*-antibonding (LUMO) orbitals of the isolated ethylene in the adsorbed geometry from the orbitals of the ethylene/metal cluster models.[31] Conclusions are given in section 5.

2. Method of Calculations

The DFT calculation was carried out by using the Gaussian 98 program[32] and the BLYP functional, which consists of the Slater exchange,[33] the Becke (B88) exhange,[34] the Vosco−Wilk−Nusair (VWN) correlation,[35] and the Lee−Yang−Parr (LYP) correlation[36] functionals. The basis sets of all the metal atoms (Cu, Ag, and Pd) were those developed by Hay and Wadt.[37] The electrons treated explicitly on Cu, Ag, and Pd are the outermost core and valence electrons ($3s^23p^63d^{10}4s^1$ for Cu, $4s^24p^64d^95s^1$ for Pd, and $4s^24p^64d^{10}5s^1$ for Cu), with the remaining core electrons treated with relativistic effective core potentials. The basis sets of the metals were contracted as (5s, 5p,5d)/[2s,2p,1d] (Cu) and (5s,6p,4d)/[2s,2p,1d] (Pd and Ag). The C and H atoms were treated with the 6-31G** basis sets. The adsorption energy E(ads) was calculated as a change in electronic energy for the adsorption of ethylene on a metal cluster, which is defined as follows:

$$E(\text{ads}) = E(\text{cluster}) + E(\text{ethylene}) - E(\text{ethylene/cluster}) \quad (1)$$

A positive E(ads) means that the adsorbate is stabilized on adsorption to a metal cluster. E(cluster) is the total energy of a bare metal cluster, E(ethylene) is the energy of the free ethylene molecule, and E(ethylene/cluster) is the energy of an ethylene/metal cluster model.

The density of states projected on an orbital, μ, of the isolated ethylene in an adsorbed geometry (PDOS$_\mu(E)$) as a function of energy is plotted by assuming a Lorentzian function with a width of $\sigma = 0.1$ eV:

$$\text{PDOS}_\mu(E) = \sum_k P_\mu^k \frac{\sigma/\pi}{(E-\epsilon_k)^2 + \sigma^2} \quad (2)$$

where ϵ_k is the energy of the kth orbital of an ethylene/metal model and the weight factor P_μ^k is the orbital population of the orbital μ in the kth orbital. P_μ^k was calculated in the following manner. First, the DFT calculation was performed on isolated ethylene in an adsorbed geometry as well as on a metal cluster to obtain the orbitals of ethylene $\{\varphi^e\}$ and the metal cluster $\{\varphi^m\}$. Because orbitals within the orbital set $\{\varphi^e \oplus \varphi^m\}$ are

not always orthogonal with each other, symmetric orthonormalization was performed to obtain an orthonormal set $\{\phi^e \oplus \phi^m\}$ by using the following equation:

$$\phi_i = \sum_j S_{ji}^{-1/2} \varphi_j \tag{3}$$

where S_{ji} is an overlap integral between φ_j and φ_i. Second, the DFT calculation was carried out to obtain the orbitals $\{\psi\}$ of the ethylene/metal cluster model by using the orthonormal set $\{\phi^e \oplus \phi^m\}$ as a basis. As a result, an orbital of the ethylene/metal cluster model ψ_k was represented by a linear combination of the orthonormal sets:

$$\psi_k = \sum_\mu c_{\mu k} \phi_\mu \tag{4}$$

Finally, the orbital population was given by

$$P_\mu^k = |c_{\mu k}|^2 \tag{5}$$

3. Ethylene/Metal Cluster Models and the Method of Structural Optimization

The Cu, Ag, and Pd substrates have a face-centered cubic (fcc) structure. The metal surfaces are modeled by two- or three-layered clusters consisting of 13−34 metal atoms. Because the calculated frequencies depend strongly on the number of metal atoms, it is crucial to employ cluster models that are large enough so that the calculated frequencies are only slightly affected by enlarging the size of the clusters if we are to obtain results that are reliable enough to be compared with the observed frequencies. Four kinds of adsorption modes are considered: (i) ethylene adsorbed on an atop bonding site with the CC bond parallel to the $\langle 1\bar{1}0 \rangle$ direction (abbreviated ST), (ii) the adsorbate on an atop bonding site with the CC bond parallel to the $\langle 100 \rangle$ direction (abbreviated LT), (iii) ethylene adsorbed on a bridge site with the CC bond parallel to the $\langle 1\bar{1}0 \rangle$ direction (abbreviated SB), and (iv) ethylene adsorbed on a bridge site with the CC bond parallel to the $\langle 100 \rangle$ direction (abbreviated LB). As illustrated in Figure 1, each of the cluster models is denoted by ETCu(SB/ST/LB/LT), followed by a series of numbers indicating the number of Cu atoms in the cluster. For example, for ETCuSB12-10-8, ethylene adsorbs on the SB site of the copper cluster with 12 metals in the first layer, 10 in the second layer, and 8 in the third layer. The geometry optimization of each ethylene/cluster model is carried out by taking all the internal degree of freedom of the adsorbate and the height of the CC bond above the first cluster plane while the metal clusters are always kept fixed at the bulk structure. (The unit cell lengths of the fcc cells are fixed at 3.615 (Cu), 4.086 (Ag), and 3.890 Å (Pd).) In all optimazation processes, the adsorbate and metal clusters are forced to have C_{2v} symmetry as a whole, which means that the CC bond is kept parallel to the surface and the adsorbate is also forced to have a mirror plane containing the CC bond and the surface normal.

4. Results and Discussion

4.1. Free Ethylene Molecule. The structural parameters optimized at the BLYP/6-31G** level and the calculated vibrational frequencies of the free ethylene molecule are compared with the corresponding experimental values in Table 1. The calculated parameters reproduce the experimental parameters well. The theoretical frequencies, which have not been scaled by any factor, are again in good agreement with the experimental frequencies. Although the theoretical frequencies are listed only for the vibrational modes observed for ethylene adsorbed on Cu(110), Ag(110), and Pd(110) (vide infra), the agreement between the theoretical and experimental frequencies for the other modes is appreciably good. These results validate the calculation at the BLYP/6-31G** level, at least for the adsorbed ethylene molecule.

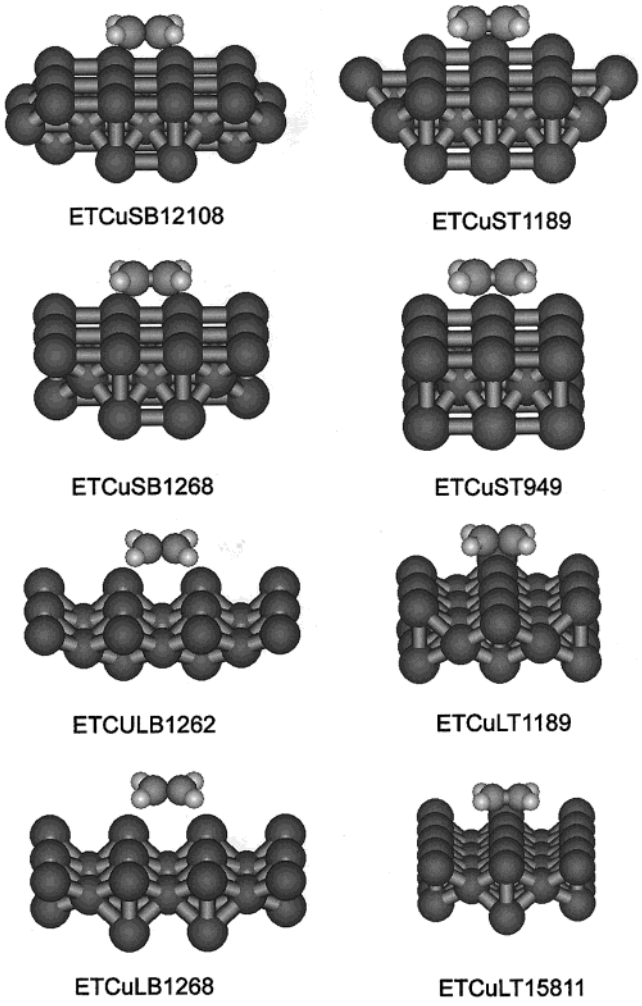

Figure 1. Cluster models for ethylene on Cu(110).

TABLE 1: Comparison between the Experimental and Calculated Values for Structural Parameters and Vibrational Frequencies

structural parameters[a]		
	experimental values[b]	theoretical values
R(CC) (Å)	1.337 ± 0.003	1.340
R(CH) (Å)	1.086 ± 0.003	1.094
A(HCH) (deg)	121.35 ± 1	121.87
T(CCH) (deg)	0.0	0.0
vibrational frequencies (cm^{-1})		
	experimental values[c]	theoretical values
ν(C═C, Ag))	1623	1659
$\gamma_s(CH_2$, Ag)	1342	1352
$\omega(CH_2, B_{1u})$	949	941

[a] R(CC) and R(CH) are the optimized values of the CC and CH distances of ethylene. A(HCH) and T(CCH) are the optimized values of the HCH angle and the dihedral angle, respectively, between the CCH planes of ethylene. [b] Taken from ref 38. [c] Taken from ref 39.

4.2. Ethylene/Cu(110). The structural parameters (R(M−C), R(CC), and T(CCH)) optimized for a series of ethylene/metal cluster models and the adsorption energies are summarized in

TABLE 2: Optimized Structural Parameters[a] and Adsorption Energies

	R(M−C) (Å)	*R*(CC) (Å)	*T*(CCH) (deg)	*E*(ads) (kJ/mol)
ETCuSB12-10-8	2.521	1.364	4.295	22.556
ETCuSB12-6-8	2.419	1.376	6.500	26.598
ETCuSB12-6	2.358	1.372	6.070	59.049
ETCuST11-8-9	2.363	1.377	5.678	45.106
ETCuST9-4-9	2.477	1.359	1.787	30.011
ETCuST9-4-5	3.441	1.343	0.445	10.164
ETCuST9-4	2.555	1.360	2.441	−32.370
ETCuLB12-6-8	3.666	1.343	0.439	11.142
ETCuLB12-6-2	3.417	1.345	0.643	0.387
ETCuLB12-6	2.880	1.352	2.591	73.324
ETCuLT15-8-11	2.428	1.363	2.416	41.188
ETCuLT11-8-9	2.476	1.360	1.943	32.331
ETCuLT9-4-9	2.477	1.359	1.787	25.030
ETCuLT9-4-5	3.558	1.343	0.287	10.164
ETAgLT15-8-11	2.846	1.353	1.377	20.964
ETAgLT9-4-9	2.907	1.351	1.008	216.512
ETAgST9-4-9	2.937	1.353	1.549	14.517
ETAgSB12-6	2.945	1.353	2.810	55.647
ETPdST9-4-9	2.319	1.396	9.508	287.906
ETPdLT9-4-9	2.295	1.395	0.449	64.178

[a] *R*(M−C) is the shortest distance between the carbon atom of ethlylene and a metal atom in the cluster, and *R*(CC) is the CC bond distance of the adsorbate. *T*(CCH) is the dihedral angle between the CCH plane of the adsorbate and the plane parallel to the top surface of the metal cluster.

Table 2. The results indicate the following: (i) The calculated adsorption energies depend on the number of metals in the clusters. The two-layered models ETCuSB12-6 and ETCuLB12-6 give abnormally large values compared to those calculated for the three-layered models in the same series. In addition, the two-layered model ETCuST9-4 gives a negative value, indicating that the adsorbate does not form a stable state, in contradiction to the experimental finding (vide infra). Thus, the two-layered models are not appropriate to the estimation of the adsorption energy. (ii) As the number of metals in the cluster models increases, the energy increases continuously for the ST and LT models, whereas the energy decreases for the SB and LB models. Although the calculated energies show a converging trend for each model, the result for the largest cluster should be considered as either a lower limit (ETCuST and ETCuLT) or an upper limit (ETCuSB and ETCuLB) to the adsorption energy. The adsorption energy is calculated for ETCuST11-8-9 to be 45.106 kJ/mol, which is in agreement with the experimental value[24] of 35−47 kJ/mol. Thus, the ST site is favored over the other sites considered, which partly conforms to the experimental results. As already explained, the photoelectron spectroscopic and diffraction studies[23,24] showed that ethylene adsorbs at either an ST or an SB site of Cu(110), whereas the STM measurements[25,26] indicated that the adsorbate occupies an SB site. (iii) As the calculated adsorption energy increases, the deviation of structural parameters *R*(CC) and *T*(CCH) from those of the free ethylene increases, which suggests that the energy increase parallels the degree of the hybridization toward the sp^3 configuration. The optimized value of *R*(CC) and the perpendicular height of the substrate above the surface (abbreviated *R*(MT), not listed in Table 2) for the SB and ST bonding states are 1.364 and 2.449 Å (ETCuSB12-10-8) and 1.377 and 2.260 Å (ETCuST11-8-9), respectively. The experimental *R*(CC) and *R*(MT) values reported by Schaff et al.[24] are 1.53 ± 0.13 and 2.09 ± 0.02 Å (SB) and 1.32 ± 0.09 and 2.08 ± 0.02 Å (ST), which are appreciably different from the optimized parameters. As explained below, the ν(CC) band for the SB bonding state of ethylene on Cu(110) is observed at 1532 cm^{-1}, and that for the ST state, at 1525 cm^{-1}. The former frequency indicates that the CC bond of the adsorbate retains appreciable double-bond nature, contradicting the experimental CC bond length, which is similar to that of a CC single bond (ca. 1.54 Å). The experimental CC bond length reported for the ST bonding state is shorter than that of the free ethylene (1.337 ± 0.003 Å, see Table 1),[38] which is also inconsistent with the observed frequency lowering from the free ethylene[39] (1623 → 1525 cm^{-1}). These results strongly suggest that the experimental parameters should be reexamined.

TABLE 3: Comparison between the Observed and Calculated Frequencies (cm^{-1}) for Cluster Models

	observed and calculated frequencies[a]		
	ν(C═C)	$\delta_s(CH_2)$	$\omega(CH_2)$
obsd frequencies[b] for ethylene/Cu(110)	1532[c]	1275[c]	909[c]
	(1525)	(1264)	
ETCuSB12-10-8	1574	1301	891
ETCuSB12-6-8	1543	1269	842
ETCuSB12-6	1556	1285	910
ETCuST11-8-9	1544	1279	865
ETCuST9-4-9	1564	1301	880
ETCuST9-4-5	1645	1347	940
ETCuST9-4	1586	1318	912
ETCuLB12-6-8	1645	1346	933
ETCuLB12-6-2	1635	1341	922
ETCuLB12-6	1610	1328	910
ETCuLT15-8-11	1584	1314	924
ETCuLT11-8-9	1594	1320	922
ETCuLT9-4-9	1596	1321	919
ETCuLT9-4-5	1645	1346	933
obsd frequencies[d] for ethylene/Ag(110)			955
ETAgLT15-8-11	1614	1334	956
ETAgLT9-4-9	1621	1337	952
ETAgSB12-6	1610	1330	941
ETAgST9-4-9	1611	1332	936
obsd frequencies[e] for ethylene/Pd(110)	1525	1235	900
ETPdST9-4-9	1519	1243	885
ETPdLT9-4-9	1533	1252	905

[a] ν(CC) and $\delta_s(CH_2)$ are CC stretching and CH_2 symmetric scissoring vibrations, which correspond to the Ag vibrational modes observed at 1623 and 1342 cm^{-1}, respectively, for free ethylene.[39] $\omega(CH_2)$ denotes a CH_2 out-of-plane wagging mode corresponding to the B_{1u} mode at 949 cm^{-1} for free ethylene.[39] [b] See ref 40. [c] Numbers indicate frequencies observed at lower coverages, and numbers in the parentheses indicate frequencies observed at higher coverages. [d] Taken from ref 22. [e] Taken from ref 29.

Table 3 lists the calculated vibrational frequencies of the optimized structures for a series of cluster models together with the experimental frequencies. The adsorbate on Cu(110) at low coverage gives the ν(CC), $\delta_s(CH_2)$, and $\omega(CH_2)$ vibrational bands at 1532, 1275, and 909 cm^{-1}, respectively, and upon increasing the coverage, the former two bands shift to 1525 and 1264 cm^{-1}, whereas the third band decreases in intensity and becomes almost unobservable.[40] The ν(CC) and $\delta_s(CH_2)$ bands correspond to the 1623 and 1342 cm^{-1} bands, respectively, of the A_g species observed for free ethylene, and the $\omega(CH_2)$ band, to the 949 cm^{-1} band of the B_{1u} species for free ethylene.[39] The frequency lowering and the appearance of the

IR-inactive modes have been ascribed to an appreciable surface−ethylene interaction.

From Table 3, it is clear that the calculated frequencies appreciably depend on the type of adsorption site, whereas the dependence of the frequencies calculated for the same site on the number of metals is not so large if the number is taken to be larger than 20. For example, the calculated frequencies for the ν(CC), $\delta_s(CH_2)$, and $\omega(CH_2)$ modes are located at 1558.5 ± 15.5, 1285 ± 16, and 866.5 ± 24.5 cm^{-1} for the SB models, 1554 ± 10 cm^{-1}, 1290 ± 11 cm^{-1}, and 872.5 ± 7.5 cm^{-1} for the ST models, 1640 ± 5 cm^{-1}, 1343.5 ± 2.5 cm^{-1}, and 927.5 ± 5.5 cm^{-1} for the LB models, and 1590 ± 6, 1317.5 ± 3.5, and 921.5 ± 2.5 cm^{-1} for the LT models. Although the dependence on the number of metals is a little larger for the SB and ST models, the results suggest that the comparison between the calculated frequencies for each adsorption site and the observed frequencies could be used to predict the adsorption site for ethylene on Cu(110). Actually, the calculated frequencies for the LB and LT models do not reproduce the observed frequencies, and there exists much better agreement between the observed frequencies and the calculated frequencies for the SB and ST models. ETCuSB12-10-8 gives the frequencies for the ν(CC), $\delta_s(CH_2)$, and $\omega(CH_2)$ modes at 1574, 1301, and 891 cm^{-1}, which compare well with the observed frequencies at 1532, 1275, and 909 cm^{-1}, respectively, for the absorbate at relatively low surface coverage.[40] This is consistent with the STM observation, which indicated that the adsorbate takes on a short bridge site with the CC bond parallel to the ⟨110⟩ direction.[25,26] However, ETCuST11-8-9 gives the ν(CC), $\delta_s(CH_2)$, and $\omega(CH_2)$ frequencies at 1544, 1279, and 865 cm^{-1}, each of which is appreciably lower than the corresponding frequency calculated for ETCuSB12-10-8. The result corresponds to the experimental fact that ethylene on Cu(110) shifts the ν(CC) and $\delta_s(CH_2)$ bands to 1525 and 1264 cm^{-1}, respectively, on increasing the surface coverage (see Table 3). Thus, the results of the calculations suggests that the frequency lowering observed for the ν(CC) and $\delta_s(CH_2)$ bands upon increasing the surface coverage can be ascribed to the conversion of the adsorption site from SB to ST. As Table 2 shows, upon conversion, the optimized CC distance (R(CC)) and twisting angle (T(CCH)) exhibit increases of 1.364 → 1.377 Å and 4.295 → 5.678°, respectively. The increase suggests a slight rehybridization toward the sp^3 configuration, which conforms to the frequency lowering of the ν(CC) and $\delta_s(CH_2)$ bands.

4.3. Ethylene/Ag(110). The results of structural optimization on a series of cluster models for ethylene on Ag(110) are listed in Table 2. Although the optimization was performed on a limited number of cluster models, the results gave some insight into the relationship between the adsorption sites and the vibrational frequencies. The calculated adsorption energies for ETAgLT15-8-11 and ETAgST9-4-9 are the same order of magnitude as the experimental value of ca. 40 kJ/mol reported by Backx et al.[41] and are appreciably smaller than the energies calculated for ETCuLT15-8-11 and ETCuST11-8-9. (The energy calculated for ETAgLT9-4-9 is abnormally large, indicating that the cluster size is too small to give a reasonable adsorption energy for the LT model.) The optimized values of the nearest Ag−C distance (R(M−C)) for the LT, ST, and SB models of ethylene on Ag(110) are appreciably larger than those for the LT, ST, and SB models of ethylene on Cu(110). The optimized structural parameters R(CC) and T(CCH) for the former models are smaller than those for the latter models. All these results indicate that ethylene molecularly adsorbs on Ag(110) and that the geometric structures of ethylene on Ag(110) are perturbed by adsorption to a lesser extent than those of the adsorbate on Cu(110). All of the studies on the adsorption structure of ethylene on Ag(110)[20,27,28] have reported that at low temperature (80−110 K) ethylene adsorbs molecularly on Ag(110) with the CC bond parallel to the surface, although the precise adsorption site has not been determined yet.

The IR spectrum of ethylene on Ag(110) exhibits the $\omega(CH_2)$ band at 955 cm^{-1}, which is appreciably higher than the $\omega(CH_2)$ frequency of the free ethylene (949 cm^{-1}). Thus, the frequency shift due to the adsorption shows an opposite trend to the case of ethylene on Cu(110), where the $\omega(CH_2)$ band shifts to the lower-frequency side (949 → 909 cm^{-1}). Table 3 lists the frequencies of the $\omega(CH_2)$ mode calculated for the cluster models of ethylene on Ag(110). From the Table, it is clear that only the LT models (ETAgLT15-8-11 and ETAgLT9-4-9) give calculated frequencies for this mode that are higher than that for free ethylene (941 cm^{-1}, see Table 1). Although the ν(CC) and $\delta(CH_2)$ frequencies have not been experimentally determined, thus hampering more reliable comparison between the experimental and theoretical frequencies, the result strongly suggests that ethylene on Ag(110) takes on the LT adsorption site.

As already explained, the ethylene−metal surface interactions have been interpreted in terms of the balance between π donation and π^* back-donation. The opposite trend in $\omega(CH_2)$ frequency shifts may reflect the difference in the balance between ethylene on Cu(110) and on Ag(110). To clarify this point and gain better insight into the difference in the ethylene−surface interaction between ethylene on Cu(110) and on Ag(110), the projections to the π-bonding and π^*-antibonding orbitals of the isolated ethylene in the asdsorbed geometries from the molecular orbitals of the ethylene/cluster modes were calculated, as explained in section 4.5.

4.4. Ethylene/Pd(110). The optimized structures and adsorption energies calculated for ETPdST9-4-9 and ETPdLT9-4-9 are listed in Table 2. The optimized R(CC) values for ethylene taking both the ST and LT sites are appreciably larger than those for the adsorbate on Cu(110) and Ag(110). The optimized T(CCH) for the ST model gives the largest value (9.508°) in Table 2. These results suggest a larger extent of sp^3 rehybridization of ethylene on Pd(110) compared to that of the adsorbate on Cu(110) and Pd(110). The energy for the ST model is much larger than that for the LT model, indicating that the adsorbate taking the ST site is more stable than that taking the LT site.

As Table 3 shows, the frequencies of the ν(CC), $\delta_s(CH_2)$, and $\omega(CH_2)$ modes calculated for ETPdST9-4-9 and ETPdLT9-4-9 are similar to each other, and the frequencies for both adsorption models reproduce the observed frequencies well. As mentioned above, however, the adsorption energy for the ST model is much larger than that for the LT model. Thus, the DFT calculation suggests that ethylene adsorbs on Pd(110), taking the ST site. This is consistent with the STM observation reported by Ichihara et al.[30]

4.5. Contribution of π Donation and π^* Back Donation to the Ethylene−Surface Interaction on Cu(110) and Ag(110). Figure 2 exhibits the density of states (PDOS) projected onto the π orbital (HOMO) and π^* orbital (LUMO) of isolated ethylene in the adsorbed geometries for ETCuSB12-10-8, ETCuST11-8-9, and ETAgLT15-8-11. The HOMO energy of each ethylene/metal cluster model, which is equivalent to the Fermi level of ethylene adsorbed on the corresponding single crystal, is indicated by a vertical line as E_F, and the energies of the π and π^* orbitals of ethylene in the adsorption geometries are given by vertical dashed lines. The comparison of the

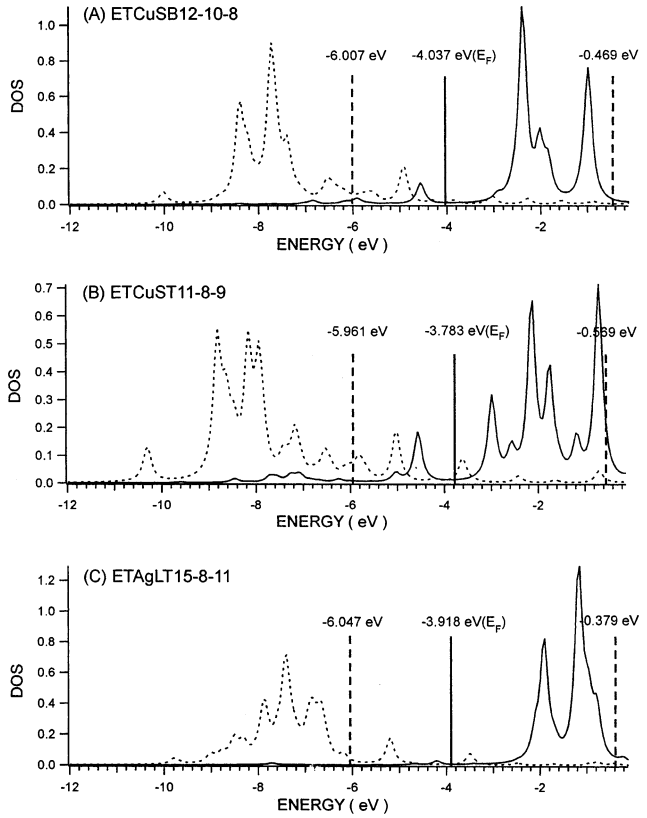

Figure 2. Projections of the π HOMO (- - -) and π^* LUMO orbitals (—) of isolated ethylene in the adsorbed geometries calculated for ethylene/Cu(110) (A, B) and ethylene/Ag(110) (C) cluster models. The solid vertical lines indicate the energy of the HOMO of the corresponding ethylene/metal cluster model (see text.) The dashed vertical lines on the left and right sides of A, B, and C indicate the energies of the π (HOMO) and π^* (LUMO) orbitals, respectively, of isolated ethylene in the adsorption geometry (see text.)

TABLE 4: Charge Transfer between Ethylene Frontier Orbitals and the Cu and Ag Clusters and the Frequency Shifts of the $\omega(CH_2)$ Band

	ETCuSB12-10-8	ETCuST11-8-9	ETAgLT15-8-11
π (HOMO)[a]	1.92	1.88	1.90
π^* (LUMO)[b]	0.15	0.28	0.03
$\Delta\nu$[c](cm^{-1})	−50 (−40)	−76	11 (7)

[a] Transferred electrons from the π orbital. [b] Back-donated electrons to the π^* orbital. [c] Calculated frequency shift of the $\omega(CH_2)$ band relative to that of the free ethylene molecule. The numbers in parentheses indicate the observed frequency shifts.[40]

projection curves of the π and π^* orbitals with the positions of the orbital energies indicates how the states are shifted in energy by adsorption. Both PDOSs are broadened over a large energy range because of overlap with metal-cluster orbitals. Bonding contributions appear below the Fermi level (E_F); the area of the π-orbital projection below E_F corresponds to the number of electrons transferred from the π orbital of the isolated ethylene to ethylene/metal-cluster orbitals, and the area of the π^*-orbital projection corresponds to the number of electrons transferred from ethylene/metal-cluster orbitals to the π^* orbital. As summarized in Table 4, the number of electrons transfer from the π orbital is 1.92 for ETCuSB12-10-8, 1.88 for ETCuST11-8-9, and 1.90 for ETAgLT15-8-11, which means that the donation of electrons from the π orbital to unoccupied metal-cluster orbitals (π donation) amounts to 0.08 for ETCuSB12-10-8, 0.12 for ETCuST11-8-9, and 0.10 for ETAgLT15-8-11. (Two electrons originally occupy the π orbital of the isolated ethylene molecule. Then, the difference between the two electrons and the amount of electron transfer from the π orbital of the ethylene/metal cluster can be considered to be the donation of electrons from the π orbital to unoccupied metal-cluster orbitals.) However, the amount of electron transfer to the π^* orbital (π^* back-donation) is 0.15 for ETCuSB12-10-8, 0.28 for ETCuST11-8-9, and 0.03 for ETAgLT15-8-11. From these results, it is clear that both of π donation and π^* back-donation play important roles in the ethylene−Cu(110) interaction, whereas π donation is the main contributor to the ethylene−Ag(110) interaction.

The calculated frequency shifts of the $\omega(CH_2)$ band relative to that of the free ethylene are also listed in Table 4. The observed shifts for ethylene on Cu(110) and Ag(110) (−40 and 7 cm^{-1}, respectively) are in good agreement with the calculated shifts for ETCuSB12-10-8 and ETAgLT15-8-11. Thus, the DFT calculation reproduces well the opposite trend of the $\omega(CH_2)$ frequency shifts for ethylene on Cu(110) and Ag(110). The IR spectra of ethylene adsorbed on Ag(110) and its atomic oxygen-reconstructed surfaces, p($n \times 1$)O−Ag(110) ($n = 6, 4, 3$), were measured by Akita et al.[21,22] They observed that the $\omega(CH_2)$ band at 955 cm^{-1} for ethylene on Ag(110) shifts to 972 cm^{-1} on the p(6×1) and p(4×1) surfaces and to 976 cm^{-1} on the p(3×1) surface, indicating that the $\omega(CH_2)$ frequency increases with the surface coverage of atomic oxygen. The desorption temperature of ethylene adsorbed on the reconstructed surfaces increases in the following order: 130 K (p(6×1)) < 145 K (p(4×1)) < 160 K (p(3×1)).[22] Thus, the stability of the adsorbate increases with the surface coverage of atomic oxygen. The electron-withdrawing nature of atomic oxygen induces positive charges on neighboring Ag atoms, resulting in an increase in the contribution of π donation as well as in the stability of the adsorbate on the surfaces. As already explained, the DFT calculation has indicated that the ethylene−Ag(110) interaction is mainly due to π donation. Thus, the results of observations and the DFT calculation suggest that in the case of ethylene on Ag(110) the frequency increase of the $\omega(CH_2)$ band relative to the corresponding frequency observed for the free ethylene molecule can be considered to be a measure of both π donation and the stability of the ethylene−surface interaction.

5. Conclusions

The DFT calculations,[8−14] which have been performed so far on ethylene/metal cluster models to clarify the adsorption modes including the adsorption energies, the optimized adsorption structures, and vibrational frequencies of ethylene, employed cluster models consisting of only a limited number of metal atoms. As explained above, the results of calculations obtained from the ethylene/metal cluster models depend strong on cluster size. Therefore, it is clear that the previous studies do not always present reliable theoretical predictions of the adsorption modes. To obtain predictions that are reliable enough to be compared with experimental results, it is crucial to employ metal clusters that are large enough so that the calculated results are only slightly affected by enlarging the cluster sizes further.

In the case of ethylene on Cu(110), which was the most extensively studied species in the present paper, the adsorption energies calculated for the ST and LT models increase with cluster size, whereas the energies for the SB and LB models decrease with cluster size (see Table 2.) Although the changes show a converging trend, the calculated energies for the largest cluster models should still be considered to be either an upper limit (for ETCuSB12-10-8 and ETCuLB12-6-8) or a lower limit

(for ETCuST11-8-9 and ETCuLT15-8-11). These limits suggest that the stability of ethylene taking on the four kinds of adsorption sites follows the order ST ≈ LT > SB > LB. As already explained, ethylene does not take the LT site, thus contradicting the predicted order of stability, which indicates the limitation of determining the stable adsorption site on the basis of adsorption energies calculated for the adsorbate/metal-cluster models. Presumably, this is partly due to the fact that the structural relaxation of the metal clusters was prohibited during the optimization processes.

However, if the number of metals is taken to be larger than approximately 20, the dependence of the frequencies calculated for the ethylene/Cu(110) cluster models on cluster size is not so large compared with that of the adsorption energies, and the calculated ν(CC), $\delta_s(CH_2)$, and $\omega(CH_2)$ frequencies for the SB, ST, LB and LT models clearly reflect each adsorption mode. Therefore, comparison of the calculated and observed frequencies allows us to conclude that ethylene on Cu(110) takes on an SB site at lower surface coverage, and upon increasing the coverage, the adsorbate changes from the SB site to ST site. These conclusions are consistent with the experimental results.[25,26]

Comparison of the optimized structural parameters of ethylene on Ag(110) with those of ethylene on Cu(110) indicated that the geometric structure of ethylene is less perturbed by the adsorption on Ag(110) than by that on Cu(110). Corresponding to this fact, the calculated ν(CC) and $\delta_s(CH_2)$ frequencies for the LT, SB, and ST models of ethylene/Ag(110) are similar to each other, and the shifts of these frequencies from those of free ethylene are smaller than those calculated for the corresponding models of ethylene/Cu(110). The characteristic feature of the IR spectrum of ethylene on Ag(110) is that the adsorbate exhibits the $\omega(CH_2)$ band at 955 cm^{-1}, which is 6 cm^{-1} higher than the band for free ethylene; this is contrasted with the cases of ethylene/Cu(110) and ethylene/Pd(110), where the bands are observed at appreciably lower frequency sites compared with that of free ethylene. The frequency increase observed for ethylene adsorbed on Ag(110) was reproduced only by the results of calculations for the LT model, which strongly suggested that ethylene takes the LT site on Ag(110).

The frequency decreases of the ν(CC), $\delta_s(CH_2)$, and $\omega(CH_2)$ bands relative to those of free ethylene due to the adsorption of ethylene on Pd(110) are larger than those on Cu(110), indicating that the perturbation proceeds further on Pd(110). Both the ST and LT models well reproduce the frequencies and the frequency shifts. The calculated adsorption energy for the former model, however, is much larger than that for the latter. On the basis of these results, it was concluded that ethylene takes the ST site on Pd(110), which is consistent with the STM observation.[30]

Thus, the analysis of the frequencies of the IR bands of ethylene on Cu(110), Ag(110), and Pd(110) by means of the DFT calculation performed on reasonably large cluster models predicts the correct adsorption site on each surface, indicating that the analysis is one of the most reliable and efficient methods to determine the adsorption site.

The calculated intensities of the IR bands by means of the DFT calculation, however, largely deviate from the experimental results. For example, the IR spectra of ethylene on Cu(110) at lower surface coverage gives rise to the ν(CC) and $\delta_s(CH_2)$ bands, the intensities of which are comparable to that of the $\omega(CH_2)$ band.[40] However, the DFT calculation for ETCuSB12-10-8 predicts the intensities of the ν(CC), $\delta_s(CH_2)$, and $\omega(CH_2)$ bands to be 0.3 (1574 cm^{-1}), 1.9 (1301 cm^{-1}) and 66.9 km/mol (891 cm^{-1}), respectively. (The numbers in parentheses indicate the calculated frequencies. See Table 3.) The appearance of the ν(CC) and $\delta_s(CH_2)$ bands, which are infrared-inactive for free ethylene with D_{2h} symmetry, are ascribable not only to the symmetry lowering due to adsorption but also to other factors such as charge-transfer interaction, which has been proposed to explain the enhancement of totally symmetric vibrations of molecular complexes such as benzene−halogen complexes[42] and the appearance of the IR bands due to ν(CC) and $\delta_s(CH_2)$ of ethylene adsorbed on mordenites.[43] Presumably, the charge-transfer effect, which cannot be treated by the DFT calculation based on the Born−Oppenheimer approximation, plays an important role in the appearance of the ν(CC) and $\delta_s(CH_2)$ bands, with the intensities comparable to that of the $\omega(CH_2)$ band.

The calculation of the PDOS of the π and π^* orbitals of isolated ethylene in the adsorbed geometries indicated that the amounts of π donation and π^* back-donation are 0.08 and 0.15 for ETCuSB12-10-8 and 0.12 and 0.28 for ETCuST11-8-9, respectively. Thus, both π donation and π^* back-donation play important roles in the ethylene−surface interaction on Cu(110). The total amount of electron transfer of 0.40 for ETCuST11-8-9 is much larger than that of 0.23 for ETCuSB12-10-8, corresponding to the larger adsorption energy (45.1 kJ/mol) of the former model compared to that (22.6 kJ/mol) of the latter. However, the amounts of π donation and π^* back-donation are 0.10 and 0.03, respectively, for ETAgLT15-8-11. Thus, only π donation plays a major role in the interaction on Ag(110).

The opposite trend in frequency shifts of the $\omega(CH_2)$ band of adsorbed ethylene compared to that of free ethylene could be ascribed to the difference in the contribution of π donation and π^* back-donation between ethylene on Cu(110) and ethylene on Ag(110). That is, the larger the frequency lowering of the $\omega(CH_2)$ band, the stronger the ethylene−surface interaction on Cu(110), and the larger the frequency increase of the band, the stronger the ethylene−surface interaction on Ag(110). It was suggested that the frequency increase is a good measure of the contribution of π donation to the interaction, where only π donation plays an important role in the interaction.

References and Notes

(1) Sheppard, N. *Annu. Rev. Phys. Chem.* **1988**, *39*, 589.
(2) Sheppard, N.; De La Cruz, C. *Adv. Catal*. **1996**, *41*, 1.
(3) Trenary, M. *Annu. Rev. Phys. Chem.* **2000**, *51*, 381.
(4) Dewer, M. S. J. *Bull. Soc. Chim. Fr.* **1951**, *18*, C79.
(5) Chatt, J.; Duncanson, L. A. *J. Chem. Soc.* **1953**, 2939.
(6) Stuve, E. M.; Madix, R. J. *J. Phys. Chem.* **1985**, *89*, 3183.
(7) Wong, Y.-T.; Hoffmann, R. *J. Chem. Soc., Faraday Trans*. **1990**, *86*, 4083.
(8) Weinelt, M.; Huber, W.; Zebisch, P.; Steinrück; Pabst, M.; Rösch *Surf. Sci.* **1992**, *271*, 539.
(9) Triguero, L.; Pettersson, G. M.; Minaev, B.; Ågren, H. *J. Chem. Phys.* **1998**, *108*, 1193.
(10) Michalak, A.; Witko, M.; Hermann, K. *J. Mol. Catal*. **1997**, *119*, 213.
(11) Fahmi, A.; van Santen, R. A. *Surf. Sci*. **1997**, *371*, 53.
(12) Bernardo, C. G. P. M.; Gomes, J. A. N. F. *J. Mol. Struct.: THEOCHEM* **2002**, *582*, 159.
(13) Kua, J.; Goddard, W. A., III. *J. Phys. Chem. B* **1998**, *102*, 9492.
(14) Watwe, R. M.; Spiewak, B. E.; Cortright, D. R.; Dumesic, J. A. *J. Catal*. **1998**, *180*, 184.
(15) Matsuura, H.; Yoshida, H. In *Handbook of Vibrational Spectroscopy*; Chalmers, J. M., Griffiths, P. R., Eds.; Wiley & Sons: New York, 2002; Vol. 3, pp 4203.
(16) Jenks, C. J.; Bent, B. E.; Bernstein, N.; Zaera, F. *Surf. Sci. Lett*. **1992**, *277*, L89.
(17) Kubota, J.; Kondo, J. N.; Domen, K.; Hirose, C. *J. Phys. Chem*. **1994**, *98*, 7653..
(18) Raval, R. *Surf. Sci*. **1995**, *331−333*, 1.
(19) Nishijima, M.; Yoshinobu, J.; Sekitani, T.; Onchi, M. *J. Chem. Phys.* **1989**, *90*, 5114.

(20) Backx, C.; de Groot, C. P. M.; Biloen, P. *Appl. Surf. Sci*. **1980**, *6*, 256.
(21) Akita, M.; Osaka, N.; Itoh, K. *Surf. Sci.* **1999**, *427*−*428*, 381.
(22) Akita, M.; Hiramoto, S.; Osaka, N.; Itoh, K. *J. Phys. Chem*. *B* **1999**, *103*, 10189.
(23) Ritz, A.; Spitzer, A.; Lüth, H. *Appl. Phys*. *A* **1984**, *34*, 31.
(24) Schaff, O.; Stampfl, A. P. J.; Hofmann, Ph.; Bao, S.; Schindler, K.-M.; Bradshaw, A. M.; Davis, R.; Woodruff, D. P.; Fritzsche, V. *Surf. Sci*. **1995**, *343*, 201.
(25) Doering, M.; Buisset, J.; Rust, H. P.; Briner, B. G.; Bradshaw, A. M. *Faraday Discuss*. **1996**, *105*, 163.
(26) Buisset, J.; Rust, H.-P.; Schweizer, E. K.; Cramer, L.; Bradshaw, A. M. *Phys. Rev*. *B* **1996**, *54*, 10373.
(27) Krüger, B.; Benndorf, C. *Surf. Sci*. **1986**, *178*, 704.
(28) Solomon, J. L.; Madix, R. J.; Stöhr, J. *J. Chem. Phys*. **1990**, *93*, 8379.
(29) Chester, M. A.; McDougall, G. S.; Pemble, M. E.; Sheppard, N. *Surf. Sci*. **1985**, *22*−*23*, 369.
(30) Ichihara, S.; Yoshinobu, J.; Ogasawara, H.; Nantoh, M.; Kawai, M.; Domen, K. *J. Electron Spectrosc. Relat. Phenom*. **1998**, *88*−*91*, 1003.
(31) Strictly speaking, the molecular orbitals in the DFT calculation should be called Kohn−Sham orbitals (KSOs). However, we use orbitals (MO) in place of KSOs hereafter to simplify the expression.
(32) Frisch, M. J.; Trucks, G. W.; Schlegel, H. B.; Scuseria, G. E.; Robb, M. A.; Cheeseman, J. R.; Zakrzewski, V. G.; Montgomery, J. A., Jr.; Stratmann, R. E.; Burant, J. C.; Dapprich, S.; Millam, J. M.; Daniels, A. D.; Kudin, K. N.; Strain, M. C.; Farkas, O.; Tomasi, J.; Barone, V.; Cossi, M.; Cammi, R.; Mennucci, B.; Pomelli, C.; Adamo, C.; Clifford, S.; Ochterski, J.; Petersson, G. A.; Ayala, P. Y.; Cui, Q.; Morokuma, K.; Malick, D. K.; Rabuck, A. D.; Raghavachari, K.; Foresman, J. B.; Cioslowski, J.; Ortiz, J. V.; Stefanov, B. B.; Liu, G.; Liashenko, A.; Piskorz, P.; Komaromi, I.; Gomperts, R.; Martin, R. L.; Fox, D. J.; Keith, T.; Al-Laham, M. A.; Peng, C. Y.; Nanayakkara, A.; Gonzalez, C.; Challacombe, M.; Gill, P. M. W.; Johnson, B. G.; Chen, W.; Wong, M. W.; Andres, J. L.; Head-Gordon, M.; Replogle, E. S.; Pople, J. A. *Gaussian 98*; Gaussian, Inc.: Pittsburgh, PA, 1998.
(33) Slater, J. C. *Phys. Rev*. **1951**, *81*, 385.
(34) Becke, A. D. *Phys. Rev*. *A* **1988**, *38*, 3098.
(35) Vosco, S. H.; Wilk, L.; Nusair, M. *Can. J. Phys*. **1980**, *58*, 1200.
(36) Lee, C.; Yang, W.; Parr, R. G. *Phys. Rev. B* **1988**, *37*, 785.
(37) Hay, P. J.; Wadt, W. R. *J. Chem. Phys*. **1985**, *82*, 299.
(38) Allen, H. C.; Plyer, E. K. *J. Am. Chem. Soc*. **1985**, *80*, 2673.
(39) Scott, A. P.; Radom, L. *J. Phys. Chem*. **1996**, *100*, 16502.
(40) The ν(CC), $\delta(CH_2)$, and $\omega(CH_2)$ frequencies are those we recorded at 80 K (unpublished work). They are almost identical to those that have been reported.[16−18]
(41) Backx, C.; de Groot, C. P. M.; Biloen, P. *Appl. Surf. Sci*. **1980**, *6*, 256.
(42) Friedrich, H. B.; Person, W. B. *J. Chem. Phys*. **1966**, *44*, 2161.
(43) Matsuzawa, H.; Yamashita, H.; Ito, M.; Iwata, S. *Chem. Phys*. **1990**, *147*, 77.